SAND2016-3023J

submitted to *Geophys. J. Int.*

Effects of linear trends on estimation of noise in GNSS position time series

K. Dmitrieva[1], P. Segall[1] and A.M. Bradley[1]

[1] *Department of Geophysics, Stanford University, Stanford, USA*

Received 2016

SUMMARY

A thorough understanding of time dependent noise in Global Navigation Satellite System (GNSS) position time series is necessary for computing uncertainties in any signals found in the data. However, estimation of time-dependent noise is a challenging task and is complicated by the difficulty in separating noise from signal, the features of greatest interest in the time series. In this paper we investigate how linear trends affect the estimation of noise in daily GNSS position time series. We use synthetic time series to study the relationship between linear trends and estimates of time-dependent noise for the six most commonly cited noise models. We find that the effects of added linear trends, or conversely de-trending, vary depending on the noise model. The commonly adopted model of random walk (RW), flicker noise (FN), and white noise (WN) is the most severely affected by de-trending, with low amplitude random walk most severely biased. Flicker noise plus white noise is least affected by adding or removing trends. Non-integer power-law noise estimates are also less affected by de-trending, but are very sensitive to the addition of trend when the spectral index is less than one. We derive an analytical relationship between linear trends and the estimated random walk variance for the special case of pure random walk noise. Overall, we find that to ascertain the correct noise model for GNSS position time series and to estimate the correct noise parameters, it is important to have good constraints on the actual trends in the data.

Key words: GNSS – noise estimation

1 INTRODUCTION

We are currently in the third decade of continuous GNSS recordings of crustal motion. Daily position time series provide highly precise estimates of GNSS velocities (Prawirodirdjo and Bock 2004; Li et al. 2012; Kierulf et al. 2014; Mantovani et al. 2016). However, the presence of time-dependent (or colored) noise in the time series complicates these estimates. First, the estimates of signals, such as linear trends, in the data can trade off with estimates of time-dependent noise. Second, the presence of time-dependent noise drastically increases the velocity uncertainty (Williams 2003), yet these noise parameters can be difficult to estimate robustly (Langbein 2012; Dmitrieva et al. 2015).

The task of estimating noise becomes easier when the signal is known. Previously we developed a network method of analyzing noise in GNSS time series from intraplate regions, where we can assume small or well characterized signals (Dmitrieva et al. 2015). Rigid plate rotations are generally well known *a priori*. In our previous analysis of data from the North American mid-continent we also corrected for trends due to glacial isostatic adjustment (GIA). We found that the noise estimate for a network of stations was unchanged after the removal of modeled linear trends due to GIA. This prompted a further investigation into the effects of linear trends on the estimates of time-dependent noise that we report on here.

From a scientific standpoint, the main interest is usually in estimating signals in the GNSS data, such as site velocities or transient signals on a variety of time scales (Miyazaki et al. 2003; Melbourne and Webb 2002). We need to quantify the time-dependent noise in the data only to calculate the uncertainty of the signal. However, estimation of a linear trend (for example) is more accurate if the noise model and amplitudes of the various noise components are accurately known. Additionally, there is considerable debate about the type and amount of noise present in GNSS data (Amiri-Simkooei 2016; Hackl et al. 2011; Santamaría-Gómez 2011; Klos et al. 2015), making it difficult to determine the true signal uncertainty. In order to correctly model noise in the data, we would ideally like to have strong *a priori* constraints on any signals present. In this paper we focus on understanding the relationship between estimated time-dependent noise and linear trends in the GNSS time series.

Time-dependent noise is usually represented by power law forms (Agnew 1992), where noise in the spectral domain is proportional to the inverse of the frequency to a power of n—the spectral index: $p \sim f^{-n}$, where n usually ranges from -1 to 3 (Agnew 1992). Some well-known cases of the power-law representation are: white noise (WN, $n = 0$), flicker noise (FN, $n = 1$) and random walk (RW, $n = 2$). However, n could be non-integer, in which case it is referred to as generic power law (PL).

There is no agreement on which noise model is the most representative of GNSS time series. Some argue for a sum of FN and WN (Williams et al. 2004; Ray et al. 2008), while others suggest that the sum of RW, FN and WN should be used (Calais et al 2006; King and Williams 2009; Amiri-Simkooei 2013; Dmitrieva et al. 2015). Finally, some suggest a sum of PL and WN (Santamaría-Gómez 2011; Klos et al. 2015; Devoti et al. 2015). Moreover, Langbein (2008) suggests that the optimal model is different for different stations. In this paper we explore the above models with synthetic time series, since knowledge of the true noise and trend allows us to precisely evaluate the effects of linear trends on estimation of the noise parameters. For every noise model and added trend we perform 100 realizations and then calculate the mean and the standard deviation of the estimated noise parameters.

There are various methods to estimate noise in GNSS time series, such as spectral estimation (Langbein and Johnson 1997; Zhang et al. 1997; Santamaría-Gómez 2011), maximum likelihood estimation (MLE) (Langbein 2004; Williams et al. 2004), least squares variance component estimation (Amiri-Simkooei 2007), applying the Allan variance of the rate to the time series (Hackl et al. 2011) and Kalman-filter-based MLE network noise estimation (Dmitrieva et al. 2015). We previously showed that when estimating time-dependent noise independently for individual stations, the time-dependent noise, especially RW, can be systematically underestimated (Dmitrieva et al. 2015). Estimating noise parameters for a network of stations simultaneously provides more robust estimates of the *average* RW variance (Dmitrieva et al. 2015). Since in this paper all data is synthetic, there are no disadvantages to estimating noise parameters for a network rather than for individual time series, as long as all time series within a network have the same noise parameters. This way we gain more precision in the estimation of lowest frequency noise (such as RW

or high-exponent PL). In order to estimate average noise parameters for a network, we modify the MLE method (Langbein 2004), calculating the likelihood of each time series having the given noise covariance, and then maximizing the sum of these likelihoods, rather than maximizing each individual likelihood:

$$-2\sum_{i=1}^{M}\mathcal{L}(x,C)=\sum_{i=1}^{M}\left[\ln(\det(C))+r_i^tC^{-1}r_i+N\ln(2\pi)\right], \quad (1)$$

where M is the number of time series in the network, C is the data covariance matrix, N is the number of observations and r_i are the residuals of the model fit for the i-th time series. To speed up the likelihood calculation we use Cholesky factorization of the covariance matrix (Bos et al. 2008).

In this paper we explore the relationship between time-dependent noise estimates and linear trends in the data. First, we present a theoretical derivation of how trends affect the estimate of RW amplitude in a case of a simple pure RW noise model. Then we look at how adding linear trends to various noise models affects the estimates of those noise parameters. Finally, we explore how noise could be perceived as trend and how removing an apparent linear trend affects the noise estimates. The main goal of this paper is to develop an understanding of how noise estimates are affected by linear trends.

2 THEORETICAL RELATIONSHIPS BETWEEN TREND AND RANDOM WALK VARIANCE

In this section we develop a theoretical relationship between trend and the estimated random walk variance. We focus on the case of pure RW and derive how the estimate of RW scale changes with the addition of a linear trend.

Let z_i be a RW, where $i = 0,\ldots,n$ is the epoch. If the period between two epochs Δt is constant, then $t_i = i\Delta t$ and $t_n \equiv T = n\Delta t$. A discrete RW process with variance $\tau^2 t$ is a cumulative sum of WN: $z_i = \tau\sqrt{\Delta t}\sum_{j=1}^{i} r_j$, where τ is the RW scale parameter with units of mm/yr$^{0.5}$ and r is a random vector with zero mean and unit variance. The difference of the series z is white noise: $z_i - z_{i-1} = \tau\sqrt{\Delta t}\ r_i$. Let $\mathrm{Diff}(\cdot)$ denote the vector of first differences and

$\mathrm{Sum}(\cdot)$ denote the sum of a vector. The expectation of the mean of the differences is 0 because the difference vector $\mathrm{Diff}(z)$ is proportional to r. Thus, the variance of the differences is

$$\mathrm{var}[\mathrm{Diff}(z)] = \mathrm{E}\left[\frac{1}{n}\mathrm{Sum}(\mathrm{Diff}(z)^2)\right] = \tau^2\Delta t, \tag{2}$$

where E denotes expected value. We obtain the simple estimator

$$\hat{\tau}^2(z) \equiv \frac{1}{n\Delta t}\mathrm{Sum}(\mathrm{Diff}(z)^2) = \frac{1}{T}\mathrm{Sum}(\mathrm{Diff}(z)^2), \tag{3}$$

whose expectation for RW z is $\mathrm{E}[\hat{\tau}^2(z)] = \tau^2$.

We now apply this estimator to the time series $y_i \equiv y(t_i) = st_i + z_i$, which is a sum of RW z and linear trend st with slope s. The time series first difference is $\mathrm{Diff}(y) = \tau\sqrt{\Delta t}\, r + s\Delta t$; therefore, the expectation of the estimator with this input is

$$\mathrm{E}[\hat{\tau}^2(y)] = \frac{1}{\Delta t}[\tau^2\Delta t + s^2\Delta t^2] = \tau^2 + s^2\Delta t. \tag{4}$$

Equation 4 gives the relationship between the scale parameter for RW and the trend in the data. Surprisingly, the estimate depends on the sampling interval. This can be understood as follows. In the limit of very sparse sampling, it is hard to distinguish between RW and a trend. With finer sampling, RW and trend become more distinct.

Figure 1 shows how the addition of a linear trend affects the RW estimate for a true RW of 1 mm/yr$^{0.5}$ and the typical Δt = 1 day. The addition of a linear trend increases the estimated RW amplitude by 2% (1.02 relative to 1 mm/yr$^{0.5}$) when the trend is 3.8 mm/yr. A 10% increase occurs when the added linear trend is 8.8 mm/yr. We also plot a numerical simulation of the estimated RW scale parameter for various trends, which agrees with the derivation above. Note that in Figure 1 the only noise in the time series is RW. Although the bias for pure RW (and daily sampling) is small, we show in the following section that this effect is larger when FN and RW are present.

In the preceding analysis, the linear trend is independent of the RW, and the expectation of the estimator $\hat{\tau}$ increases. De-trending has the opposite effect. De-trending adds a linear trend that is correlated with the RW. The expectation of $\hat{\tau}$ decreases. This can be understood by a derivation similar to that in Equation 4 for simple de-trending procedures. For example, suppose a linear trend is removed such that a time series y_i starts and ends at 0. Then the slope $s = -z_n/T$ (the maximum likelihood estimate for pure RW errors), and thus $y_i = z_i - z_n t_i/T$. Proceeding as

before, we construct the first difference $\mathrm{Diff}(y)$:

$$y_i - y_{i-1} = \tau\sqrt{\Delta t}\left[r_i - \frac{z_n}{T}\Delta t\right] \tag{5}$$

$$= \tau\sqrt{\Delta t}\left[r_i - \frac{\sum_{j=1}^{n} r_j}{T}\Delta t\right] \tag{6}$$

$$= \tau\sqrt{\Delta t}\left[\left(1 - \frac{\Delta t}{T}\right) r_i - \frac{\Delta t}{T}\sum_{j=1, j\neq i}^{n} r_j\right]. \tag{7}$$

Then the expectation of the estimator is

$$\mathrm{E}[\hat{\tau}^2] = \frac{1}{T}\mathrm{E}\left[\mathrm{Sum}(\mathrm{Diff}(y)^2)\right] \tag{8}$$

$$= \frac{\tau^2\Delta t}{n\Delta t}\sum_{i=1}^{n}\mathrm{E}\left[\left(1 - \frac{\Delta t}{T}\right) r_i - \frac{\Delta t}{T}\sum_{j=1, j\neq i}^{n} r_j\right]^2 \tag{9}$$

$$= \frac{\tau^2}{n}\sum_{i=1}^{n}\left[\left(1 - \frac{\Delta t}{T}\right)^2 \mathrm{E}[r_i^2] + \left(\frac{\Delta t}{T}\right)^2 \sum_{j=1, j\neq i}^{n}\mathrm{E}[r_j^2]\right]. \tag{10}$$

In the second line, we used $T = n\Delta t$. In the third line, we used $\mathrm{E}[r_i r_j] = 0$ when $i \neq j$ to remove all terms in $r_i r_j$, $i \neq j$. Now we use $\mathrm{E}[r_i^2] = 1$ to finish:

$$\mathrm{E}[\hat{\tau}^2] = \frac{\tau^2}{n}\sum_{i=1}^{n}\left[\left(1 - \frac{\Delta t}{T}\right)^2 + \left(\frac{\Delta t}{T}\right)^2 (n-1)\right] \tag{11}$$

$$= \tau^2\left[\left(1 - \frac{\Delta t}{T}\right)^2 + \left(\frac{\Delta t}{T}\right)^2 (n-1)\right] \tag{12}$$

$$= \left(1 - \frac{\Delta t}{T}\right)\tau^2. \tag{13}$$

Equation 13 should be compared with Equation 4. In Equation 4, there is a term $s^2\Delta t$ in addition to τ^2; in Equation 13, there is instead a term $-\tau^2\Delta t/T$, from which we can identify $s = -\tau/\sqrt{T}$. Again, while the bias is small for pure RW, we show that it can be considerably larger when FN and WN are present.

While it is possible to derive an analytical expression for pure RW, when any other noise component is added to the noise model it appears not to be possible to derive closed-form expressions for the expected value of the noise parameter. Instead, we explore the effects of linear trends on the estimates in the next section using synthetic data.

3 EMPIRICAL RELATIONSHIP BETWEEN TRENDS AND NOISE ESTIMATES

In this section we perform tests of a more realistic noise scenarios for GNSS position time series. We use synthetically generated time series consisting of a sum of time-dependent and white noise. Since there is no general agreement on which noise model is the most appropriate for GNSS time series, we consider three commonly used noise models, as discussed in the introduction. The inferred noise parameters depend on the topocentric components analyzed, with horizontal components of GNSS positions being more precise than the vertical. We explore a range of noise amplitudes based on estimates reported in the literature. The first model we consider is a sum of RW, FN (4 mm/yr$^{0.25}$) and WN (1 mm), with three RW amplitudes: 1, 0.5 and 0.1 mm/yr$^{0.5}$. Secondly, we consider a sum of PL (amplitude of 3 mm/yr$^{0.25n}$ and two different spectral indices $n = 1.4$, which lies between RW and FN, and $n = 0.3$, which lies between FN and WN) and WN (1 mm). Lastly, we consider a sum of FN of 4 mm/yr$^{0.25}$ and WN of 1 mm.

First, we investigate how adding various linear trends affects the estimated time-dependent noise. For each scenario we generate a network of 4 time series each with 10 years of daily data, fixed noise, and different linear trends varying from 0 to 1 mm/yr with an increment of 0.1 mm/yr. Then we estimate noise parameters assuming no trend, and compare the means and standard deviations of the estimates (Figure 2). The top panel shows the mean and standard deviation of the estimates of the RW scale parameter for the RW+FN+WN model. As expected smaller amplitudes of RW are most affected by the addition of a linear trend. When RW is high (1 mm/yr$^{0.5}$), the mean estimate of RW amplitude exceeds the true value by one standard deviation when linear trend is 0.52 mm/yr (dashed line) and exceeds the true value by 10% (1.1 mm/yr$^{0.5}$) when the linear trend is equal to 0.63 mm/yr. For RW of 0.5 mm/yr$^{0.5}$, the mean estimate exceeds the true value by one standard deviation when the trend exceeds 0.27 mm/yr (dashed line) and is over the true value by 10% (0.55 mm/yr$^{0.5}$) once the linear trend is 0.34 mm/yr. In the case of low RW of 0.1 mm/yr$^{0.5}$, adding even 0.13 mm/yr of trend causes the mean to exceed the true value by one standard deviation. In summary, when the RW variance is large moderate trends do not significantly affect the RW amplitude estimate, while low level RW can be strongly influenced by the presence of a trend in the data. Note also that the mean of the RW estimates in all three cases approaches a common

value when the trends exceed ~ 1 mm/yr, suggesting that for sufficiently large trend the site velocity dominates the estimated RW. We do not show the corresponding FN or WN estimates, as they are not greatly affected by the addition of linear trends for the range of parameters tested.

The second panel of Figure 2 shows the means and standard deviations of the spectral index n for the PL+WN noise model. We consider two cases, first, the PL+WN model with high spectral index $n = 1.4$ and then with very low index $n = 0.3$. We estimate both the spectral index and the amplitude of the PL component, but only show the estimates of n, since it is significantly more affected by the added trend. Figure 2 shows that adding a linear trend affects noise with $n = 0.3$ much more than noise with $n = 1.4$. For $n = 1.4$ the mean of the estimate exceeds the true value by one standard deviation once the linear trend is 0.37 mm/yr (dashed line) and it exceeds the true n by over 10% only for trends exceeding 1 mm/yr. For $n = 0.3$ adding even 0.1 mm/yr of trend causes the mean estimated n to exceed the true value by over 50%. As with the RW+FN+WN model, the estimates of the spectral index converge when a sufficiently large trend is added.

The bottom panel of Figure 2 shows how the presence of a linear trend affects the estimates of FN amplitude in a FN+WN model. We find that even with a 1 mm/yr trend, the mean estimate still does not exceed 10% of the true FN amplitude. The mean of the FN amplitude estimate exceeds the true value by one standard deviation when the linear trend is 0.4 mm/yr (dashed line), but in this case this results mainly from the small standard deviation in the estimate (there are fewer parameters estimated compared to previous models).

We next consider how de-trending affects the estimates of noise parameters. This is important because long period noise could be interpreted as a trend. Using synthetic data we calculate a mean of the absolute values of the estimated apparent trend for all six noise scenarios explored in this paper. We emphasize that for these estimates the time series consisted only of noise and no trend. The results for 10 years of daily positions time series are shown in Table 1. The calculations show that a significant trend could be estimated when there is in fact no underlying linear signal. The apparent linear trend is greater for models with noise with higher spectral indices, such as RW and high n PL, but is still present for FN+WN. This emphasizes how time-dependent noise affects both the velocity estimate as well as the uncertainty in that estimate.

We again use synthetic tests to explore the impact of de-trending on estimates of time-dependent noise parameters. For each scenario we generate a network of 4 time series with 10 years of daily data, fixed noise parameters, but with no linear trend. We use linear least squares with the appropriate data covariance to estimate and remove apparent trends, then estimate noise parameters from the residuals.

For the RW+FN+WN model (Figure 3), in the case of high RW (1 mm/yr$^{0.5}$) removing a linear fit significantly biases the RW estimate. One third of the tests have zero estimated RW amplitude, while the remaining two thirds have non-zero estimates but are still biased to low values. For moderate RW (0.5 mm/yr$^{0.5}$) 90% of the estimated scale parameters are zero following trend removal. The mean estimate of RW amplitude is only 0.06 mm/yr$^{0.5}$. Initially, we estimate and remove both the slope and the intercept of the linear trend, since this is more conventional. However, we found that removing just the slope produces a different result (Figure 3, bottom panel). Subtracting the small intercept brings the estimate of RW down. Even when we remove just the apparent trend (without the intercept), the RW amplitude is underestimated, the mean estimate of RW is now 0.2 mm/yr$^{0.5}$ and almost half the estimates are now at 0 mm/yr$^{0.5}$. Thus, for the RW+FN+WN model, removing an apparent linear trend leads to a significant underestimation of the RW amplitude. This bias leads to an underestimation of velocity uncertainty (Table 2). We do not show estimates of FN and WN amplitudes as they are not strongly affected by de-trending for this noise model.

For the case of PL+WN model (Figure 4), for both low and high spectral index, n is just slightly underestimated after removal of a fitted trend. For $n = 1.4$ the mean estimate before de-trending is 1.40, while it is 1.38 after de-trending. For $n = 0.3$ prior to de-trending the mean estimate is 0.30 and $n = 0.28$ after the trend is removed. There is no change in the estimate of the amplitude of the PL or WN amplitudes for the PL+WN model. For FN+WN model (Figure 5) there is almost no change in the FN estimate. Before de-trending the mean estimate is 4.00 mm/yr$^{0.25}$ and it is 3.98 mm/yr$^{0.25}$ after de-trending.

4 DISCUSSION

Our findings show that the degree to which signals, such as linear trends, affect the estimates of time-dependent noise parameters varies depending on the underlying noise model. We provide a derivation that shows that linear trends with small to moderate slopes do not significantly affect the estimate of noise parameters for the case of pure RW. Of course, it is unrealistic to assume pure RW as a noise model for actual GNSS time series. We also tested six different noise models that are more appropriate for GNSS noise. When considering these noise models we find that adding linear trends may significantly impact the estimated noise parameters.

To better understand the dependence of the noise estimate on the linear trend consider the power spectra plotted in Figure 6, which shows theoretical noise components: RW, FN, WN, their sum and a linear trend. At high frequencies the noise is mainly affected by WN, in the mid-frequencies FN is dominant, while RW only dominates for a limited band-width at the lowest frequencies. Figure 6 also shows that a linear trend has a slope of -2, as does RW. (Although both trend and RW have the same slope in the amplitude domain the phasing is very different, which is clear in the time domain). With realistic amounts of FN and WN, RW only dominates at the lowest frequencies, making it harder to estimate and more likely to trade-off with trend.

To test this we compared the affects of adding a linear trend to the RW+FN+WN model for typical and very low amplitude FN. Based on the spectral plots, we expect that with very low FN the added trend would lead to a smaller bias in the RW estimate. Indeed, Figure 7 shows that with the very low FN adding 1 mm/yr linear trend increases the RW estimate by only $\sim 50\%$, whereas with typical FN amplitude the RW estimate is biased by $\sim 260\%$ of the true value.

A perhaps counterintuitive result is that for pure RW noise, the sampling frequency determines how much a trend biases the noise estimate (equation 4). Perhaps some insight can be gained by considering the limiting case of two data points at the beginning and end of the time series. In this limit the RW time series is indistinguishable from a linear trend. As the sampling interval decreases the difference time series for RW approaches a fixed distribution (in this case Gaussian white noise), whereas the difference series for the trend is a constant, $s\Delta t$. Thus a ML estimator can better differentiate trend from RW even though their amplitude spectra are similar.

Our simulations show that time-dependent noise can be incorrectly perceived as a linear trend. Removing this apparent, but non-existent, trend may bias the noise estimate to low values; RW noise is especially sensitive to de-trending. For the RW+FN+WN model de-trending can significantly decrease estimates of RW amplitude. Removing a linear trend also decreases the estimate of the spectral index for PL+WN model, but to a lesser extent. Removal of an apparent trend does not affect the estimate of FN for the FN+WN model, in part because of the difference in spectral slope between the trend (-2) and FN (-1). In contrast to the PL model, the spectral index is fixed when estimating noise parameters for the FN+WN model.

For the RW+FN+WN model de-trending can result in very low and even null estimates of RW, even when the true RW amplitude is significant. Figure 8 shows a power spectral plot of one of the cases from Figure 3B—that is, an individual time series for the RW+FN+WN model—with moderate RW (0.5 mm/yr$^{0.5}$). Prior to de-trending, the RW was estimated correctly at 0.48 mm/yr$^{0.5}$, however after de-trending the estimate of RW scale parameter is zero. Figure 8 illustrates that at the lowest frequencies, where RW dominates, the spectrum is similar to that of a linear trend. If the best fitting trend is removed, the FN+WN model becomes a good fit to the residual time series. This helps explain how de-trending can bias the RW estimate. We also note that in this paper we maximize the sum of the likelihoods from multiple time series. We have previously shown that network approaches are more precise at estimating low levels of RW (Dmitrieva et al. 2015). When maximizing the likelihood for each time series, as typically done, de-trending is even more likely to result in null estimates of RW. We conclude that de-trending the data can lead to biased or even vanishing RW estimates. At the same time, accurately estimating weak RW is difficult in the presence of trends. The estimated RW amplitudes can be significantly larger than the true values, when unaccounted for trends are present. Hence, one has to be very careful about de-trending the time series, since this could lead to either completely neglecting or significantly overestimating the RW variance.

The FN+WN model is insensitive to both moderate linear trends as well as to de-trending. With strong *a priori* knowledge that FN+WN is the correct noise model, one could be somewhat liberal with removing trends. The same holds for the PL+WN model, as we observe that de-trending

only weakly biases estimates of the spectral index. For PL indices that lie between RW and FN, such as $n = 1.4$, adding even moderate trends does not have a significant effect on the estimate of the spectral index. However, for PL noise with lower spectral index, such as $n = 0.3$, even a very small (e.g. 0.05 mm/yr) trend has a significant effect on the estimate of the spectral index. Removing a linear trend for low index PL noise does not affect the estimate of the index. Hence, if one is confident in the PL+WN model and maximum likelihood estimates of spectral index are low, it is fair to assume that those estimates are accurate. However, higher spectral index estimates could be due to 1) the index actually being high, 2) a residual linear trend or 3) PL+WN not being the correct model to use.

It is important to note that there is independent evidence that GNSS monument motion contributes RW to geodetic time series (Wyatt 1989; Johnson and Agnew 1995). We have shown that de-trending can lead to null estimates of RW, potentially leading to the erroneous conclusion that a simpler FN+WN model, that requires only 2 parameters to estimate, is more appropriate. The best solution to this problem may be to analyze data from areas where it is known *a priori* that there are no linear-in-time signals in the time series, or where the trends are well-known. Such areas could be the interiors of plates far from plate-boundary deformation, and also far from large GIA signals, or where such effects are well modeled. As noted in the Introduction, preliminary work in the North American mid-continent found that removing GIA velocities barely influenced estimates of noise parameters (Dmitrieva et al. 2015). In that case, the average GIA signals for the horizontal time series were low, with a mean of 0.28 mm/yr, and the estimated RW was relatively high, 1 mm/yr$^{0.5}$.

5 CONCLUSIONS

When a small to moderate linear trend is added to a pure RW time series with daily sampling, the effects of the trend on the estimates of RW variance are minor. However for more realistic noise models, the results vary significantly depending on the noise model. In the presence of WN and FN, RW is both very sensitive to de-trending as well as un-modeled residual trends. It is difficult to either confirm or reject the presence of RW in the data without knowing *a priori* the true signal

trend. Both FN+WN and PL+WN (with the PL spectral index $1 < n < 2$) models are relatively insensitive to de-trending. However, for the PL+WN model with lower spectral indices $0 < n < 1$, an added trend drastically increases the estimate of the spectral index.

Estimates of time-dependent noise depend on knowledge of any linear trends present in the data. In order to know the uncertainties of the estimated linear trends we need to know the time-dependent noise model and variances. At the same time to accurately estimate the noise we need to know any trends in the data. To break out of this loop we need additional information. To determine the best noise model and typical variances in the actual GNSS position time series we recommend focusing on areas where trends are either small or well-known *a priori*.

ACKNOWLEDGMENTS

This work was supported by NASA under the NASA Earth and Space Science Fellowship Program - Grant 14-EARTH14R-47 (double-check), (SCEC?)

REFERENCES

Agnew, D.C., 1992. The time-domain behavior of power-law noises. *Geophys. Res. Lett.,* **19(4)**, 333-336.

Amiri-Simkooei, A.R., Tiberius, C.C.J.M. and Teunissen, S.P., 2007. Assessment of noise in GPS coordinate time series: methodology and results. *J. geophys. Res.,* **112(B7)**.

Amiri-Simkooei, A.R., 2013. On the nature of GPS draconitic year periodic pattern in multivariate position time series. *J. geophys. Res.,* **118(5)**, pp.2500-2511.

Amiri-Simkooei, A.R., 2016. Non-negative least-squares variance component estimation with application to GPS time series. *J Geod.*, **89(6)**, 591–606.

Bos, M.S., Fernandes, R.M.S., Williams, S.D.P. and Bastos, L., 2008. Fast error analysis of continuous GPS observations. *J Geod.*, **82(3)**, 157–166.

Calais, E., Han, J.Y., DeMets, C. and Nocquet, J.M., 2006. Deformation of the North American plate interior from a decade of continuous GPS measurements. *J. geophys. Res.,* **111(B6)**.

Devoti, R., Pietrantonio, G., Pisani, A. R. and Riguzzi, F., 2015. ermanent GPS Networks in Italy: Analysis of Time Series Noise *Part of the series International Association of Geodesy Symposia*, 1-8.

Dmitrieva, K., Segall, P. and DeMets, C., 2015. Network-based estimation of time-dependent noise in GPS position time series. *J Geod.*, 1-16.

Johnson, H.O. and Agnew, D.C., 1995. Monument motion and measurements of crustal velocities. *J. geophys. Res.,* **22(21)**, 2905-2908.

Hackl, M., Malservisi, R., Hugentobler, U. and Wonnacott, R., 2011. Estimation of velocity uncertainties from GPS time series: Examples from the analysis of the South African TrigNet network. *J. geophys. Res.,* **116(B11)**.

Kierulf, H.P., Steffen, H., Simpson, M.J.R., Lidberg, M., Wu, P. and Wang, H., 2014. A GPS velocity field for Fennoscandia and a consistent comparison to glacial isostatic adjustment models. *J. geophys. Res.,* **119(8)**, 6613-6629.

King, M.A. and Williams, S.D., 2009. Apparent stability of GPS monumentation from short?baseline time series. *J. geophys. Res.,* **114(B10)**.

Klos, A., Bogusz, J., Figurski, M. and Gruszczynski, M., 2015. Error analysis for European IGS stations. *Studia Geophysica et Geodaetica*, 1-18.

Langbein, J., 2012. Estimating rate uncertainty with maximum likelihood: differences between power-law and flickerrandom-walk models. *J. geophys. Res.,* **86(9)**, 775-783.

Langbein, J., 2004. Noise in two?color electronic distance meter measurements revisited. *J. geophys. Res.,* **109(B4)**.

Langbein, J., 2008. Noise in GPS displacement measurements from Southern California and Southern Nevada. *J. geophys. Res.,* **113(B5)**.

Langbein, J. and Johnson, H., 1997. Correlated errors in geodetic time series: Implications for time?dependent deformation. *J Geod.*, **102(B1)**, 591-603.

Li, Q., You, X., Yang, S., Du, R., Qiao, X., Zou, R. and Wang, Q., 2012. A precise velocity field of tectonic deformation in China as inferred from intensive GPS observations. *Science China Earth Sciences*, **55(5)**, 695-698.

Mantovani, E., Viti, M., Cenni, N., Babbucci, D. and Tamburelli, C., 2015. Present Velocity Field in the Italian Region by GPS Data: Geodynamic/Tectonic Implications. *International Journal of Geosciences*, **6(12)**, 1285.

Melbourne, T.I. and Webb, F.H., 2002. Precursory transient slip during the 2001 Mw= 8.4 Peru earthquake sequence from continuous GPS. *J. geophys. Res.,* **29(21)**.

Miyazaki, S.I., McGuire, J.J. and Segall, P., 2003. A transient subduction zone slip episode in southwest Japan observed by the nationwide GPS *J. geophys. Res.,* **108(B2)**.

Prawirodirdjo, L. and Bock, Y., 2004. Instantaneous global plate motion model from 12 years of continuous GPS observations. *J. geophys. Res.,* **109(B8)**.

Ray, J., Altamimi, Z., Collilieux, X. and van Dam, T., 2008. Anomalous harmonics in the spectra of GPS position estimates. *GPS solutions*, **12(1)**, 55-64.

Santamaría-Gómez, A., Bouin, M.N., Collilieux, X. and Wöppelmann, G., 2011. Correlated errors in GPS

position time series: implications for velocity estimates. *J. geophys. Res.,* **116(B1)**.

Williams, S. D. P., 2003, The effect of coloured noise on the uncertainties of rates estimated from geodetic time series. *J Geod.*, **76(9-10)**, 483–494.

Williams, S.D., Bock, Y., Fang, P., Jamason, P., Nikolaidis, R.M., Prawirodirdjo, L., Miller, M. and Johnson, D.J., 2004. Error analysis of continuous GPS position time series. *J. geophys. Res.,* **102(B8)**.

Wyatt, F., 1989. Displacement of surface monuments- Vertical motion. *J. geophys. Res.,* **94** 1655-1664

Zhang, J., Bock, Y., Johnson, H., Fang, P., Williams, S., Genrich, J., Wdowinski, S. and Behr, J., 1997. Southern California Permanent GPS Geodetic Array: Error analysis of daily position estimates and site velocities. *J. geophys. Res.,* **109(B3)** 18035-18055.

Table 1. Average (over 1000 estimations for each value) of absolute value of estimated linear trend in the synthetic time series (10 years of daily data) that consist only of noise.

Noise model	Mean trend (mm/yr)
RW(1 mm/yr$^{0.5}$)+FN(4 mm/yr$^{0.25}$)+WN(1 mm)	0.30
RW(0.5 mm/yr$^{0.25}$)+FN(4 mm/yr$^{0.25}$)+WN(1 mm)	0.18
RW(0.1 mm/yr$^{0.25}$)+FN(4 mm/yr$^{0.25}$)+WN(1 mm)	0.12
PL(n=1.4, 3 mm/yr$^{0.075}$)+WN(1 mm)	0.21
PL(n=0.3, 3 mm/yr$^{0.35}$)+WN(1 mm)	0.02
FN(4 mm/yr$^{0.25}$)+WN(1 mm)	0.11

Table 2. Velocity uncertainty with the RW+FN+WN model, where FN is 4 mm/yr$^{0.25}$, WN is 1 mm and RW amplitude as shown in the table.

Random walk, mm/yr$^{0.5}$	1.4	1.0	0.5	0.1	0
Velocity uncertainty, mm/yr	0.5	0.35	0.21	0.13	0.13

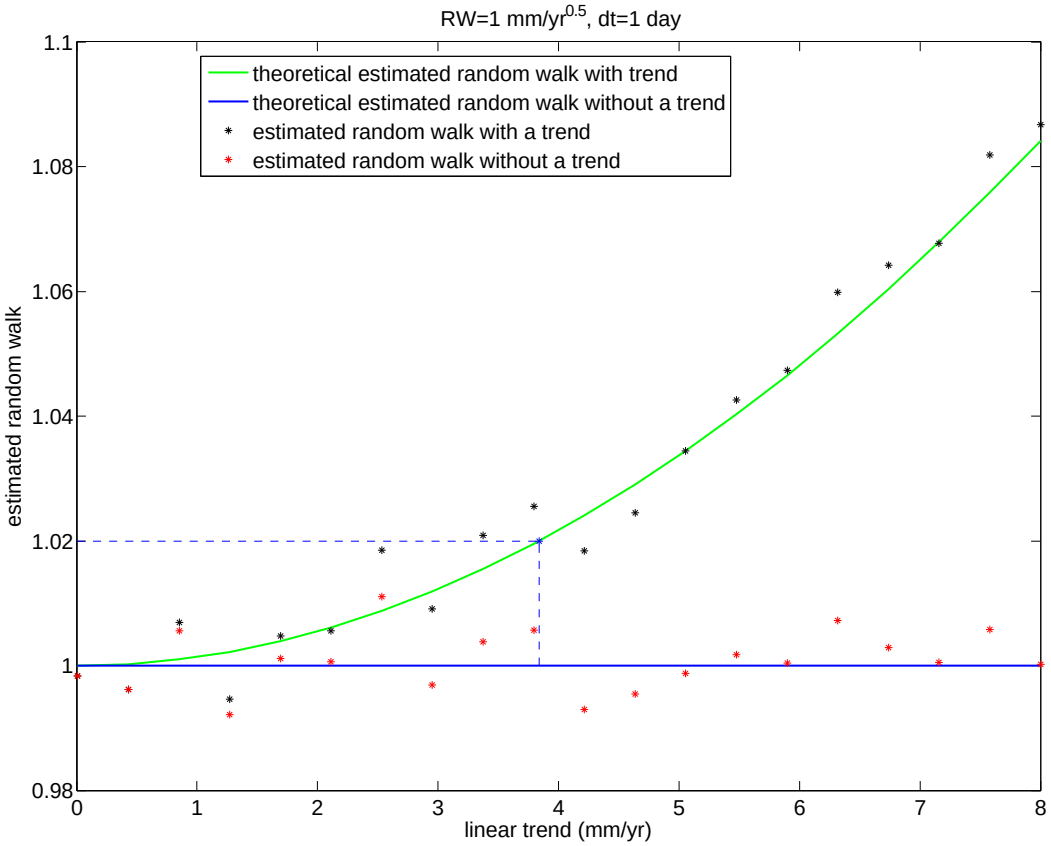

Figure 1. The effect of a linear trend on the RW estimate. Solid lines represent the theoretical RW estimate (Equation 4) for pure RW (blue) and RW + linear trend (green). Dots show simulations (each dot is a mean of 100 runs): red dots are estimates of RW amplitude for time series of pure RW and black dots are RW amplitude estimates for time series of a sum of RW and linear trend. Blue dashed lines show where the error in the RW estimate exceeds 2%, which for RW of 1 mm/yr$^{0.5}$ and daily sampling rate equals 3.8 mm/yr.

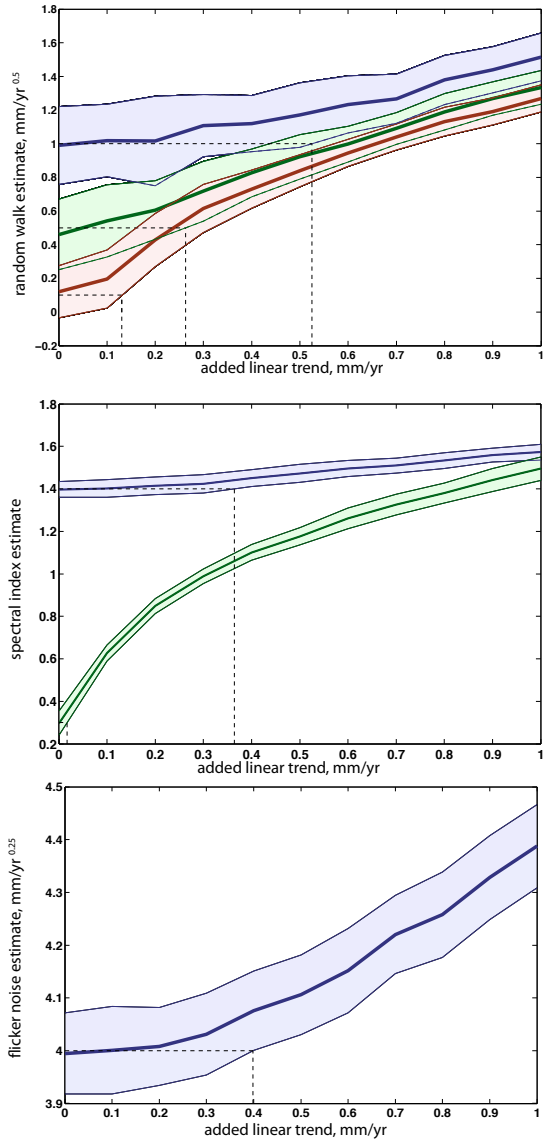

Figure 2. Changes in estimated noise parameters due to the presence of a linear trend in the data. For each experiment, we create 4 time series containing the same amount of noise sampled daily for 10 years. A linear trend is added, with values ranging from 0 to 1 mm/yr, with an increment of 0.1 mm/yr. The estimated noise parameters are shown assuming that the data contain noise only. Each combination of noise model, noise amplitude and trend, is repeated 100 times. The mean (thick lines) and standard deviation (thin lines) of the estimates are shown. Top: the noise model is RW+FN+WN, the true RW is 1 mm/yr$^{0.5}$ for the purple curves, 0.5 mm/yr$^{0.5}$ for the green curves and 0.1 mm/yr$^{0.5}$ for the pink curves. Middle: PL (3 mm/yr$^{0.25n}$ amplitude and spectral index $n = 1.4$ (blue) and $n = 0.3$ (green))+WN model. Bottom: FN (4 mm/yr$^{0.25}$)+WN. The dashed lines show where the mean of the estimates exceeds the true value by one standard deviation.

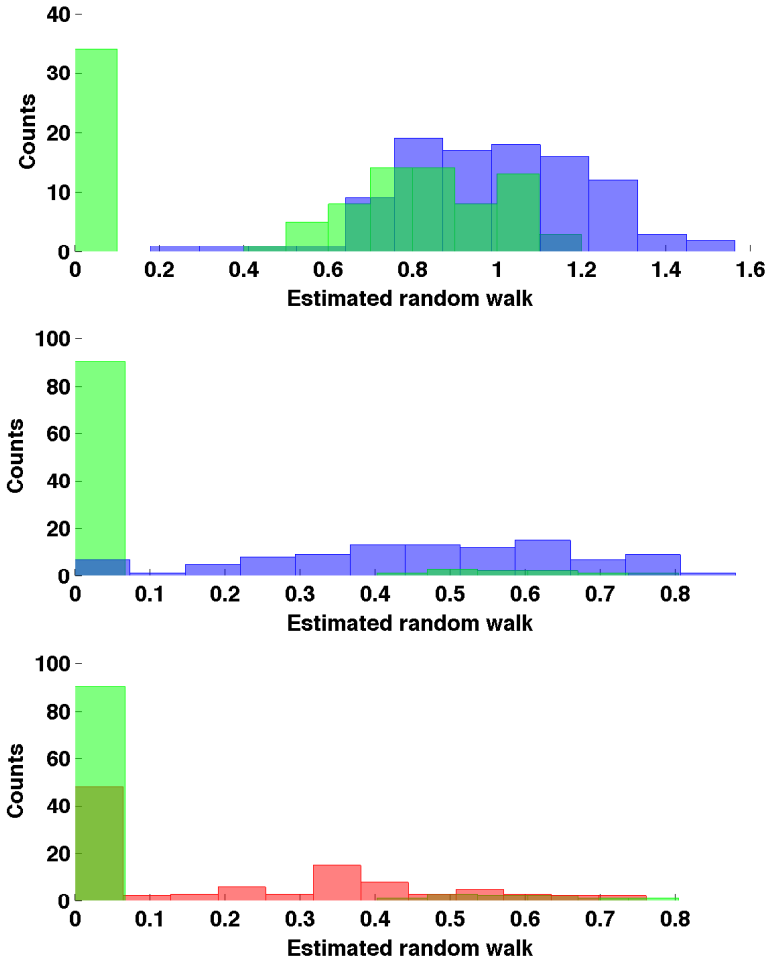

Figure 3. Effects of de-trending on noise estimates (RW+FN+WN model). Synthetic time series contain RW + FN + WN (all panels have the same FN 4 mm/yr$^{0.25}$ and WN 1 mm), RW from top: 1 mm/yr$^{0.5}$, mid and bottom: 0.5 mm/yr$^{0.5}$. The apparent trend is subtracted and then noise parameters are estimated. Histograms show the distribution of estimated RW amplitude for 100 trials. Blue - original, Green - de-trended (intercept and slope removed), Red - de-trended (just the slope removed).

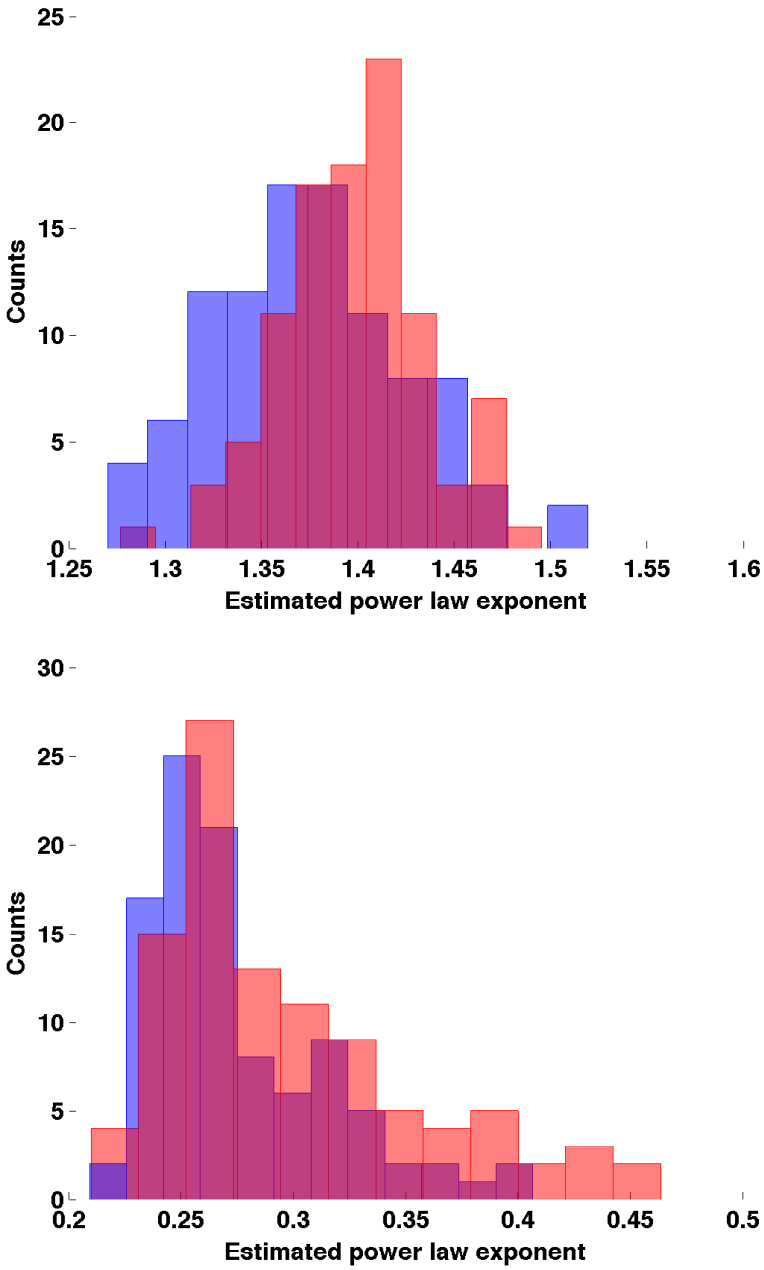

Figure 4. Effects of de-trending on noise estimates (PL+WN model). Synthetic time series contain PL 3 mm/yr$^{0.5n}$ with $n = 1.4$ (top) and $n = 0.3$ (bottom) and WN 1 mm. The apparent trend is subtracted and then noise parameters are estimated. Here we show histograms of the distribution of PL spectral index estimates for 100 trials. Red - original, Blue - de-trended.

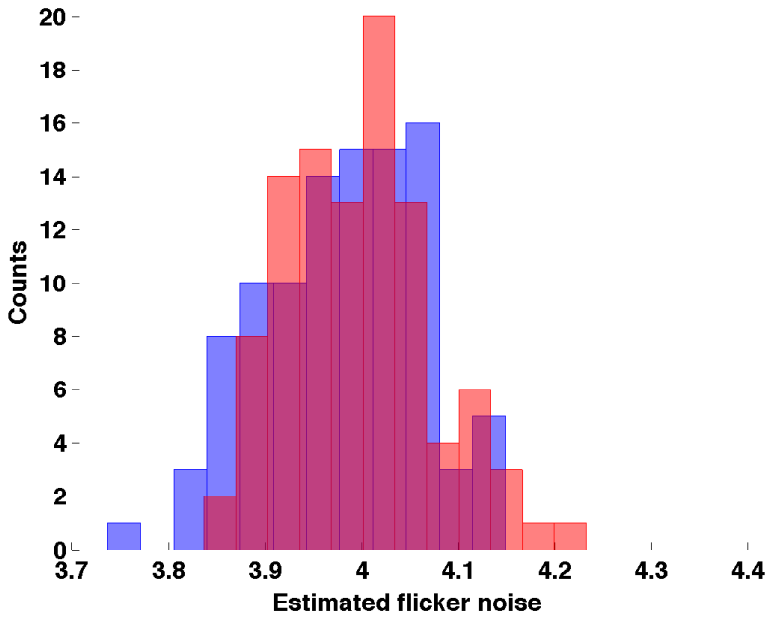

Figure 5. Effects of de-trending on noise estimates (FN+WN model). Synthetic time series contain FN 4 mm/yr$^{0.25}$ and WN 1mm. The apparent trend is subtracted and then noise parameters are estimated. Here we show histograms of the distribution of FN amplitude estimates for 100 trials. Red - original, Blue - de-trended.

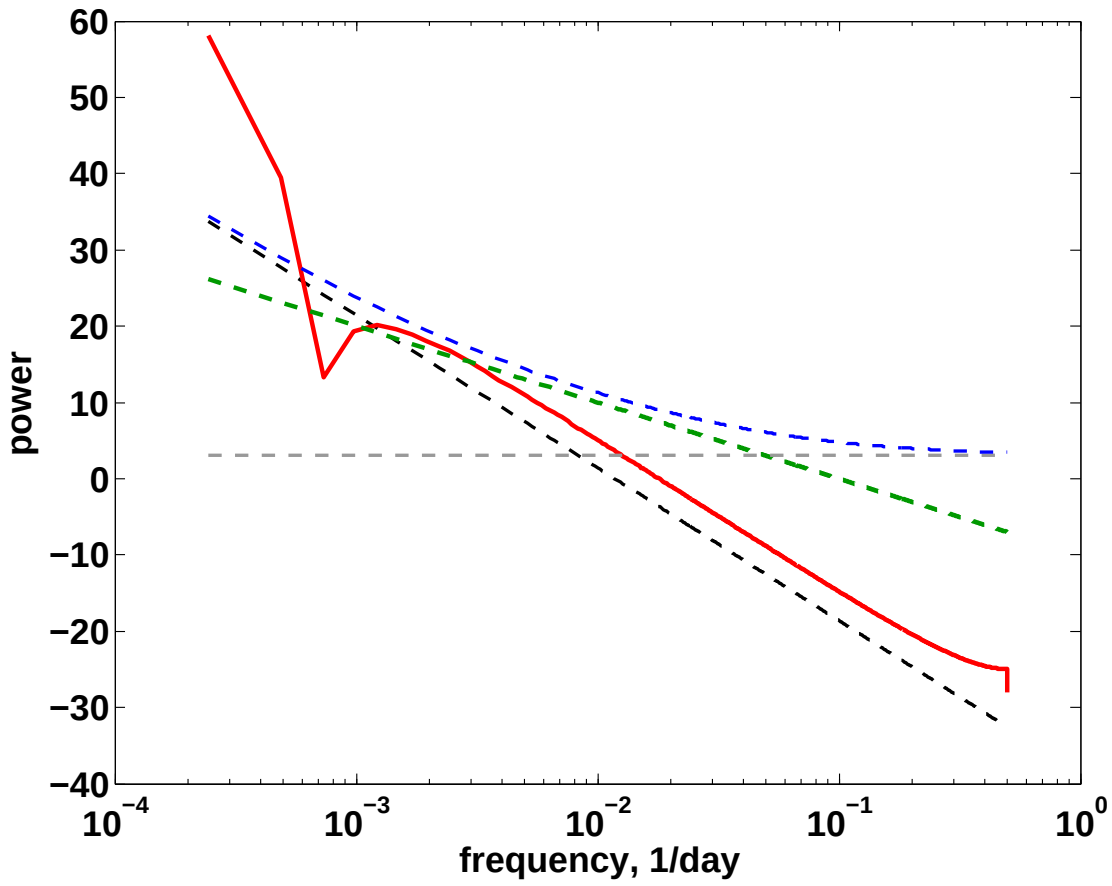

Figure 6. Power spectra showing the relationship between various noise components and a linear trend. Theoretical slope for 1 mm/yr$^{0.5}$ RW (black), 4 mm/yr$^{0.25}$ FN (green) and 1 mm WN (grey). The blue dashed line is a sum of RW, FN and WN. The red line is a power spectrum of 10 years of daily data with slope of 3.8 mm/yr.

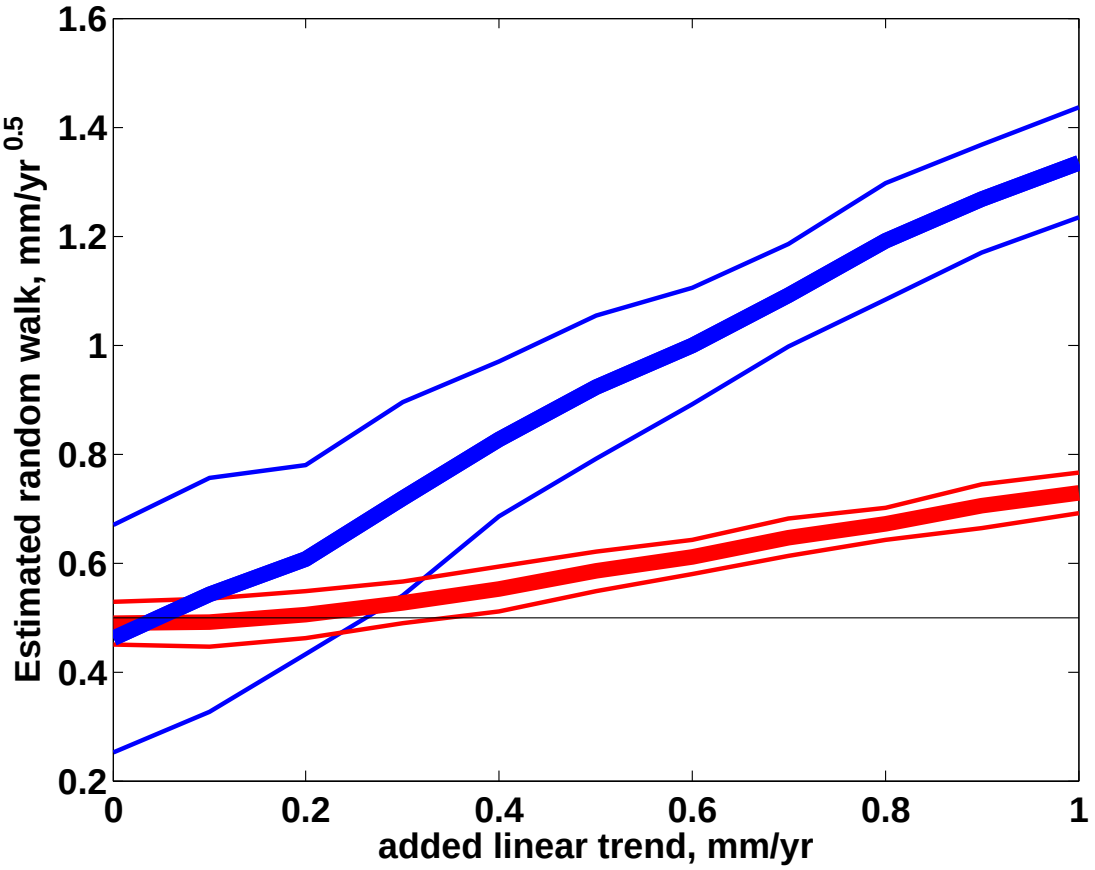

Figure 7. Comparison of the effects of added linear trend on RW estimates, for RW+FN+WN with typical (4 mm/yr$^{0.25}$, in blue) and very low (0.1 mm/yr$^{0.25}$, in red) FN. For both cases RW is 0.5 mm/yr$^{0.5}$ and WN is 1 mm. Thick lines indicate the mean of 100 estimates and thinner lines are one standard deviation. Black line shows true RW.

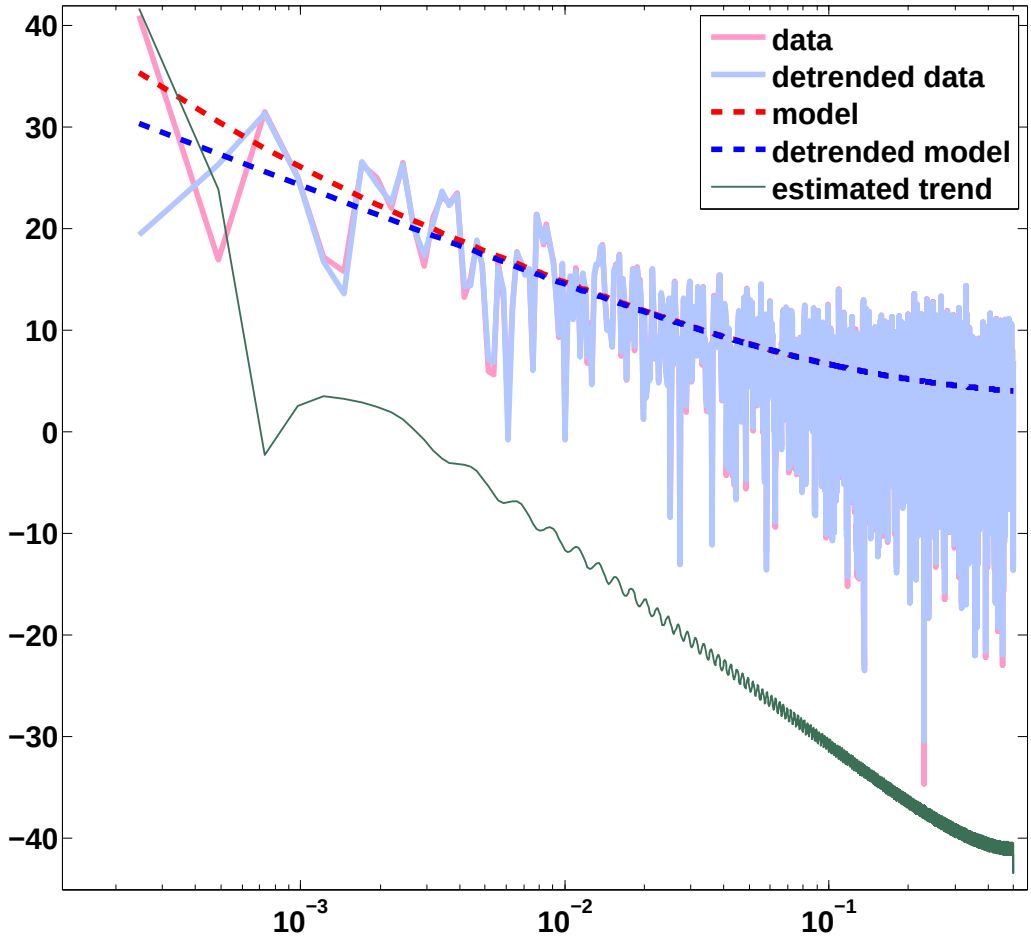

Figure 8. Illustration of how de-trending effects RW estimates in the spectral domain. Pink line is a power spectrum of a synthetically generated time series that is a sum of RW, FN and WN. Red dashed line is the model used to generate the time series (RW of 1 mm/yr$^{0.5}$, FN of 4 mm/yr$^{0.25}$ and WN of 1 mm). Light blue line is the power spectrum of the same time series de-trended. Dark blue dashed line is the model prediction based on the noise estimates of the de-trended time series (estimated RW of 0 mm/yr$^{0.5}$). Green curve is the power spectrum of the fitted trend.